Laser and Particle Beams (2000), *18*, 269–273. Printed in the USA.

2D numerical modeling of pulsed plasma acceleration by a magnetic field

A.A. KONDRATYEV

Russian Federal Nuclear Center—All-Russia Institute of Technical Physics (RFNC VNIITF), P.O. Box 245, Snezhinsk, Chelyabinsk region, 456770 Russia

(Received 19 May 1999; Accepted 19 May 1999)

Abstract

Pulsed plasma guns are used to obtain high-velocity (10^7–10^8 cm/s) plasma flows. Their performance is restricted by an instability of the plasma acceleration by a magnetic field. This paper presents results of a 2D numerical study of plasma dynamics in the plasma gun. The ZENIT-2D code solving the magnetohydrodynamic (MHD) equations on a fixed Eulerian mesh is used. The plasma parameters and geometry are chosen to be close to the parameters of the MK-200 installation (Sidnev *et al.*, 1983). The influence of the initial distribution of a neutral gas on accelerator performance is investigated. A brief description of the code and details of the simulations are presented. It is shown that the instability of acceleration leads to turbulent mixing of the plasma and magnetic field and, correspondingly, to a broader current channel than that predicted by the classical diffusion with the Spitzer conductivity. Numerical results are compared with experimental data (Bakhtin & Zhitlukhin, 1998) displaying a good qualitative agreement.

1. INTRODUCTION

Plasma acceleration by a pulsed magnetic field is very widely used: *Z*- and Θ-pinches, plasma focus devices, plasma flow switches, and different types of plasma guns. The main common feature of these devices is the MHD instability of acceleration. Potter (1971) likely was the first to perform 2D modeling of pulsed plasma acceleration in the axial direction between coaxial electrodes. Those calculations used a uniform initial density distribution with a faster movement along the internal electrode because the magnetic pressure is higher there ($P_M \propto r^{-2}$). This principally differs from the radial acceleration in pinches because in the latter case, the instability appears because of initial disturbances to the plasma parameters. Also, acceleration in such a system differs from the acceleration in a compact toroid device (see, e.g., Raman *et al.*, 1993) stabilized by the poloidal magnetic field frozen in the plasma. As a result of faster movement along the internal electrode, the radial component of the magnetic pressure appears and pushes the plasma to the external electrode, so that plasma accumulates near the external electrode having low axial velocity. The plasma pressed by the magnetic field to the external electrode is relatively stable, because the magnetic field lines have a favorable curvature. A nonuniform density distribution may substantially change plasma acceleration if the Alfven velocity is higher inside the interelectrode gap. In this case there is the plasma near the internal electrode that is unstable because of an unfavorable curvature of the magnetic field lines. As a result of the instability, the plasma fills like jets the interelectrode gap, closes it, and accelerates. This causes turbulent mixing of the plasma and the magnetic field with formation of a wide current channel. The experiments conducted by Bakhtin and Zhitlukhin (1998) show that the current is distributed over the length of ≈10 cm that substantially exceeds the estimate of the diffusion length with the Spitzer conductivity.

Numerical calculations of pulsed plasma acceleration in a plasma gun face difficulties caused by the MHD instability and a large ratio between the acceleration length and the skin depth. The Lagrangian codes are inapplicable because of strong deformations and mixing. The Eulerian codes face difficulties related to accurate description of a plasma-vacuum boundary and numerical diffusion, especially of the magnetic field into the plasma. One must use a large computational mesh in the Eulerian codes if the ratio between the acceleration length and the skin depth is large.

The ZENIT-2D code and details of the calculations are described in the next section. Section 3 considers the prob-

Address correspondence and reprint requests to: Presently Scientist at the Division of Theoretical Physics and Applied Mathematics, RFNC VNIITF, PO Box 245, Snezhinsk, Chelyabinsk region, 456770, Russia. E-mail: a.a.kondratyev@vniitf.ru

lem with typical configuration and parameters and proves applicability of the model. Calculated results are presented in Section 4.

2. CODE ZENIT-2D

The ZENIT-2D code solves the equations of MHD with heat conductivity of ions and electrons and magnetic field diffusion. They include the continuity, momentum, energy and Maxwell equations:

$$\frac{\partial \rho}{\partial t} + \mathrm{div}(\rho \mathbf{v}) = \mathbf{0}, \tag{1}$$

$$\frac{\partial(\rho \mathbf{v})}{\partial t} + \nabla(\rho \mathbf{v}\mathbf{v}) + \nabla(\mathrm{P_i} + \mathrm{P_e}) = \frac{\mathrm{rot}\mathbf{B} \times \mathbf{B}}{4\pi}, \tag{2}$$

$$\frac{\partial}{\partial t}(\rho \epsilon_e) + \mathrm{div}(\rho \epsilon_e \mathbf{v}) + \mathrm{P_e}\,\mathrm{div}\,\mathbf{v} = \mathrm{div}(\kappa_e \nabla T_e) + \eta \mathbf{j}^2 + Q_{ei}, \tag{3}$$

$$\frac{\partial}{\partial t}(\rho \epsilon_i) + \mathrm{div}(\rho \epsilon_i \mathbf{v}) + \mathrm{P_i}\,\mathrm{div}\,\mathbf{v} = \mathrm{div}(\kappa_i \nabla T_i) - Q_{ei}, \tag{4}$$

$$\mathbf{j} = \frac{c}{4\pi}\mathrm{rot}\mathbf{B}, \quad \frac{\partial \mathbf{B}}{\partial t} = \mathrm{rot}[\mathbf{v} \times \mathbf{B}] - \frac{c^2}{4\pi}\mathrm{rot}(\eta\,\mathrm{rot}\mathbf{B}), \tag{5}$$

In this problem, only B_φ is a nonzero component of the magnetic field. The electrical current I in the plasma gun is determined by the capacitive energy store (generator) and described by the equations:

$$C\frac{dU_C}{dt} = -I, L\frac{dI}{dt} = U_C - U_p - RI. \tag{6}$$

$$U_p I = \oint \mathbf{W}\, d\mathbf{S}, \ \mathbf{W} = \frac{c}{4\pi}[\mathbf{E} \times \mathbf{B}]. \tag{7}$$

Here, L, C, R, U_C are inductance, capacity, resistance, and capacity voltage of the generator. The Saha equations are used to qualitatively consider the average charge of ions

$$Z\frac{Z_k}{Z_{k-1}} = 6.06 \cdot 10^{21}\frac{g_k}{g_{k-1}}\frac{T_e^{3/2}}{n}\exp(-I_{k-1}/T_e). \tag{8}$$

We use the equations of state (EOS) of the perfect plasma including the energy of ionization. The transport coefficients are calculated using the formulas of Braginskii (1965).

A Eulerian orthogonal nonuniform fixed computational mesh is used. The components of the velocity vector are defined on the cell interfaces, other variables are in the cell center. Solving the system of the equations is split into steps with respect to physical processes: At first the MHD equations without heat conductivity and magnetic field diffusion (ideal MHD) are solved, then magnetic field diffusion and heat conductivity for a motionless matter are solved. The equations of the ideal MHD are solved in two stages:

1. The equations are solved in Lagrangian coordinates (no fluxes through cell interfaces). The numerical schemes with explicit and implicit pressure and magnetic field are used.
2. Results of the first stage are used to calculate fluxes of mass, momentum, and full (kinetic and internal) energy through fixed interfaces of the cells. Then results for the new time level are derived from the conservation laws. To calculate the fluxes, we use two methods: (1)—the first order donor cells method, and (2)—the second order spatial low phase error flux corrected transport (LPE FCT) method (Boris & Book, 1976).

The equations for the electrical circuit in Eqs. 6 and 7 and magnetic field diffusion in Eq. (5) are solved simultaneously. The equation of diffusion is solved by the implicit method of Yanenko (1967). The heat conductivity equations for ions and for electrons accounting for Joule heating and ionization in Eq. (8) are solved self-consistently using the implicit method of Yanenko (1967) and Newton's linearization.

In the process of plasma acceleration, the plasma density drops to the values at which the MHD approximation is not satisfied and the Alfven velocity $\mathrm{v_A} = B/\sqrt{4\pi\rho}$ strongly restricts the time step if the scheme with the explicit magnetic pressure is used. To solve this problem the critical value of the plasma density ρ_V, as in the work of Potter (1971), is set. If the plasma density in a cell is lower than ρ_V, then in this cell the coefficients of heat and electrical conductivity are set to zero (this is a "vacuum" cell).

The accurate boundary conditions must take into account the processes on the electrodes. These are formation of an electrostatic layer in presence of a magnetic field and accurate calculations of the heat and particle fluxes from the plasma to the electrode in this layer, vaporization of the electrode including heat conductivity in it and subsequent ionization of the vapor. Solution of this problem by the 2D MHD modeling demands high computational resources and has not been used in these calculations. The electrodes are considered as rigid walls and the losses of mass and energy are set to zero.

3. GEOMETRY AND TYPICAL PARAMETERS OF THE PROBLEM

The calculations have been conducted for the parameters of the experimental installation MK-200 (Sidnev *et al.*, 1983; Bakhtin & Zhitlukhin, 1998) sketched in Figure 1. Working gas (H) is in the valve of the volume 30 cm^3 under the pressure of 80–90 atm. At a fixed time the valve opens and the gas begins filling the gap between the electrodes through the holes in the internal electrode. In a fixed period after the opening of the valve, the capacitive energy store (capacity of 1140 μF, inductance of 30 nH, resistance of 10^{-3} Ohm, charge voltage of 20–25 kV) switches on.

The typical time of plasma acceleration is $\sim$10 μs, the length in the axial direction is $\sim$1 m, and the distance be-

https://doi.org/10.1017/S0263034600182163 Published online by Cambridge University Press

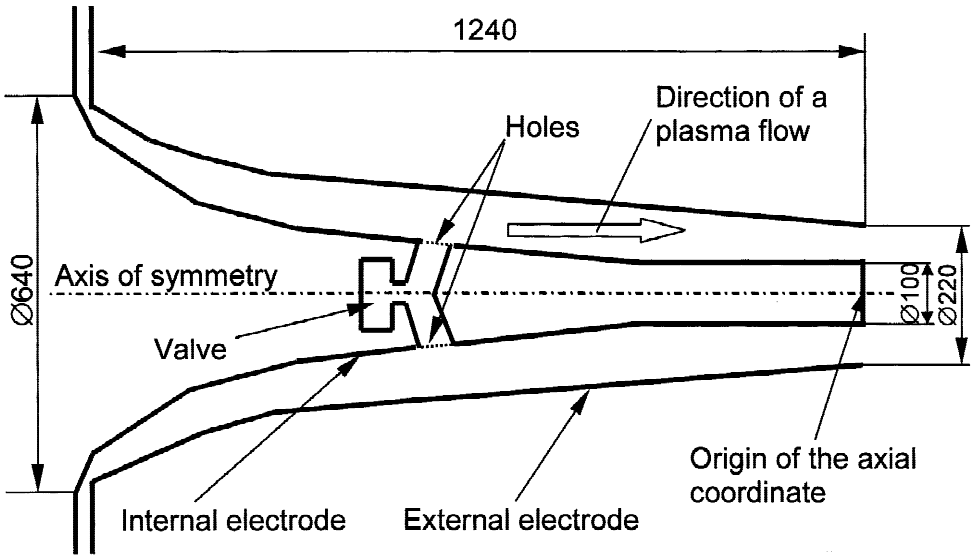

Fig. 1. Sketch of the MK-200 plasma gun (Bakhtin & Zhitlukhin, 1998). Sizes are in mm.

tween the electrodes is ~10 cm. The typical values in the current channel (by order of magnitude) are as follows: density $\sim 10^{18}$ cm^{-3}, temperature ~10 eV, velocity $\sim 10^7$ cm/s, and magnetic field $\sim 10^4$ Gs. Correspondingly, the plasma parameters are: the electron collision time $\tau_e \sim 10^{-12}$ s, the ion collision time $\tau_i \sim 10^{-10}$ s, the time of electron-ion temperature equalization $\tau_{ei} \sim 10^{-9}$ s, the coefficient of temperature conduction without magnetization $\sim 10^5$ cm^2/s, the skin depth ~0.1–1 cm, and the current velocity $|u| = |v_i - v_e| \sim 10^6$ cm/s. Therefore, the MHD approximation is valid (except the region behind the current channel from which the plasma is pushed by a magnetic field and which is considered as a "vacuum", that is, the coefficients of the heat and electrical conductivity are set to zero). The small value of the electron–ion temperature time equalization allows application of a one-temperature model (electron and ion temperatures are equal). The small value of the temperature conductivity coefficient allows neglecting of heat conductivity. The comparative calculations carried out with and without heat conductivity have showed a good agreement of the results. That is why all the rest calculations have been carried out without heat conductivity. The current velocity is considerably smaller than the mass velocity ($|u| \ll |v_e|$, $|v_i| \sim 10^7$ cm/s), therefore the Hall terms may be neglected.

4. RESULTS OF THE CALCULATIONS

The density distribution of molecular hydrogen calculated for the parameters of the MK-200 installation is shown in Figure 2. The axial coordinate origin is shown in Figure 1. There are the density maxima near the holes in the internal electrode, near the external electrode connected with the gas flow reflection from it and two peaks near the internal electrode at some distance from the holes due to the secondary reflection. This density distribution has been used as initial data for the calculations of the plasma acceleration by a magnetic field. The uniform computational mesh with the cell size $\Delta z = 2$ mm and $\Delta r = 1$ mm has been used. The value of the critical "vacuum" density ρ_V has been set to $5 \cdot 10^{15}$ cm^{-3}

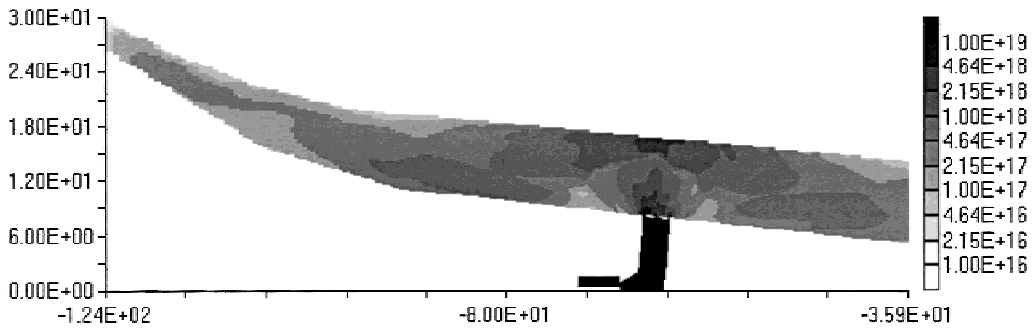

Fig. 2. Distribution of the molecular hydrogen density (cm^{-3}) at 300 μs after opening of the valve (only the part of the computational geometry is shown).

https://doi.org/10.1017/S0263034600182163 Published online by Cambridge University Press

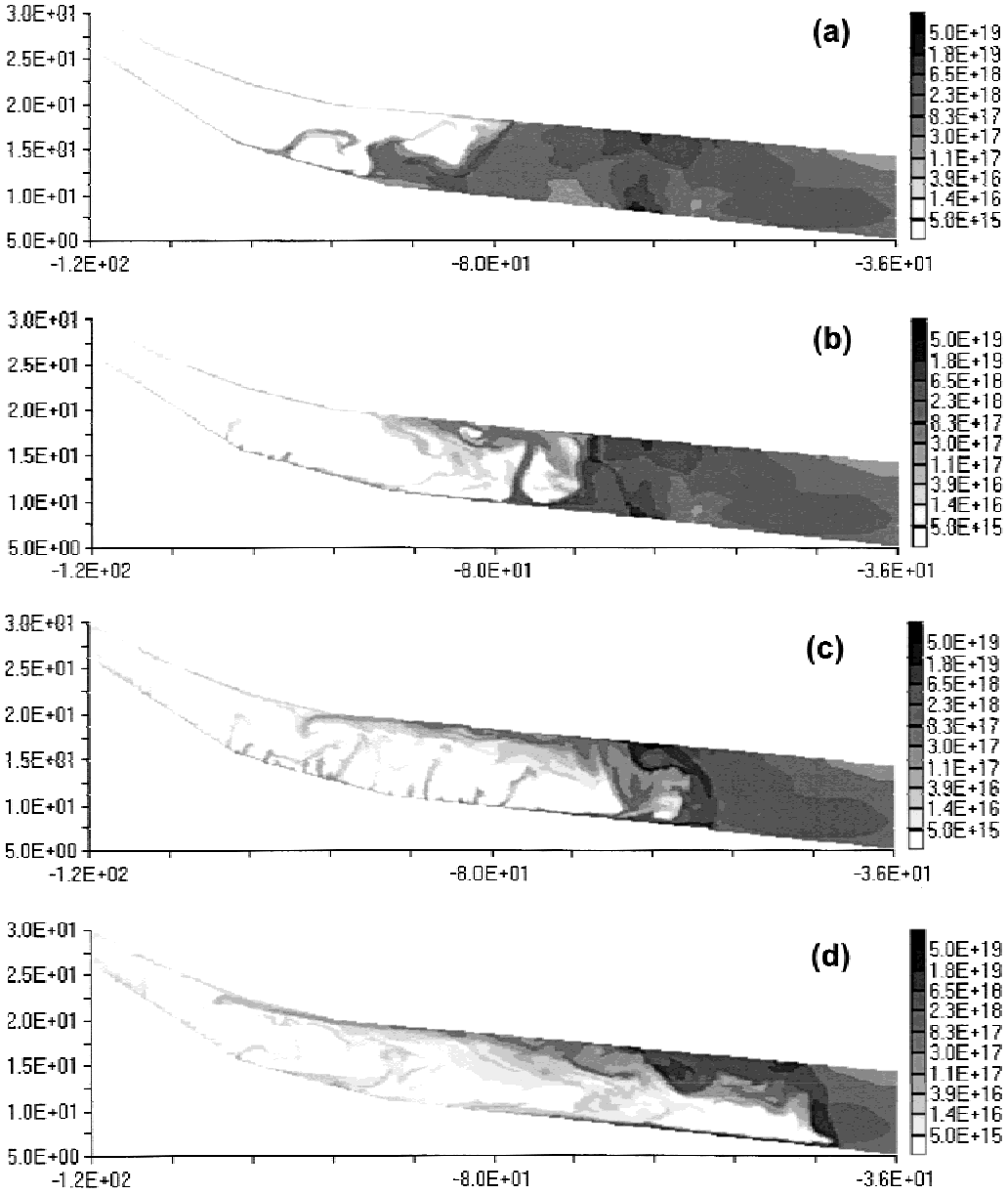

Fig. 3. Distribution of the plasma density (cm^{-3}) at the times: (a) 5 μs, (b) 7.5 μs, (c) 10 μs, and (d) 12.5 μs.

in these calculations. Comparative calculations conducted for other values of ρ_V show the same results. Initial current has been established in one radial strip of zones on the back of the plasma.

The results of the plasma dynamics calculations are shown in Figures 3 and 4. The nonuniform density distribution results in a faster movement inside the interelectrode gap of the accelerator leaving some part of the plasma near the internal electrode (it is clearly seen for the time 5 μs). The plasma pressed by the magnetic field to the internal electrode is unstable because of an unfavorable curvature of the magnetic field lines. As a result of the MHD instability the plasma begins like jets filling the gap between the electrodes, closes it, and accelerates. This MHD instability near the internal electrode leads to turbulent mixing of the plasma and the magnetic field and results in a broader current channel than that predicted by diffusion with the Spitzer conductivity (this is distinctly seen for the times 7.5 and 10 μs). This result agrees with the experimental measurements conducted by the magnetic probes (Bakhtin & Zhitlukhin, 1998). Like in the case with the uniform density distribution, there is a large amount of the plasma near the external electrode having the velocity approximately 10 times lower than in the current channel. The instability near the internal electrode also may lead to fast penetration of impurities from the evaporated electrode material into the accelerated plasma. The plasma velocity at the time 5 μs is approximately 8 cm/μs. At the time 7.5 μs and 10 μs the plasma

https://doi.org/10.1017/S0263034600182163 Published online by Cambridge University Press

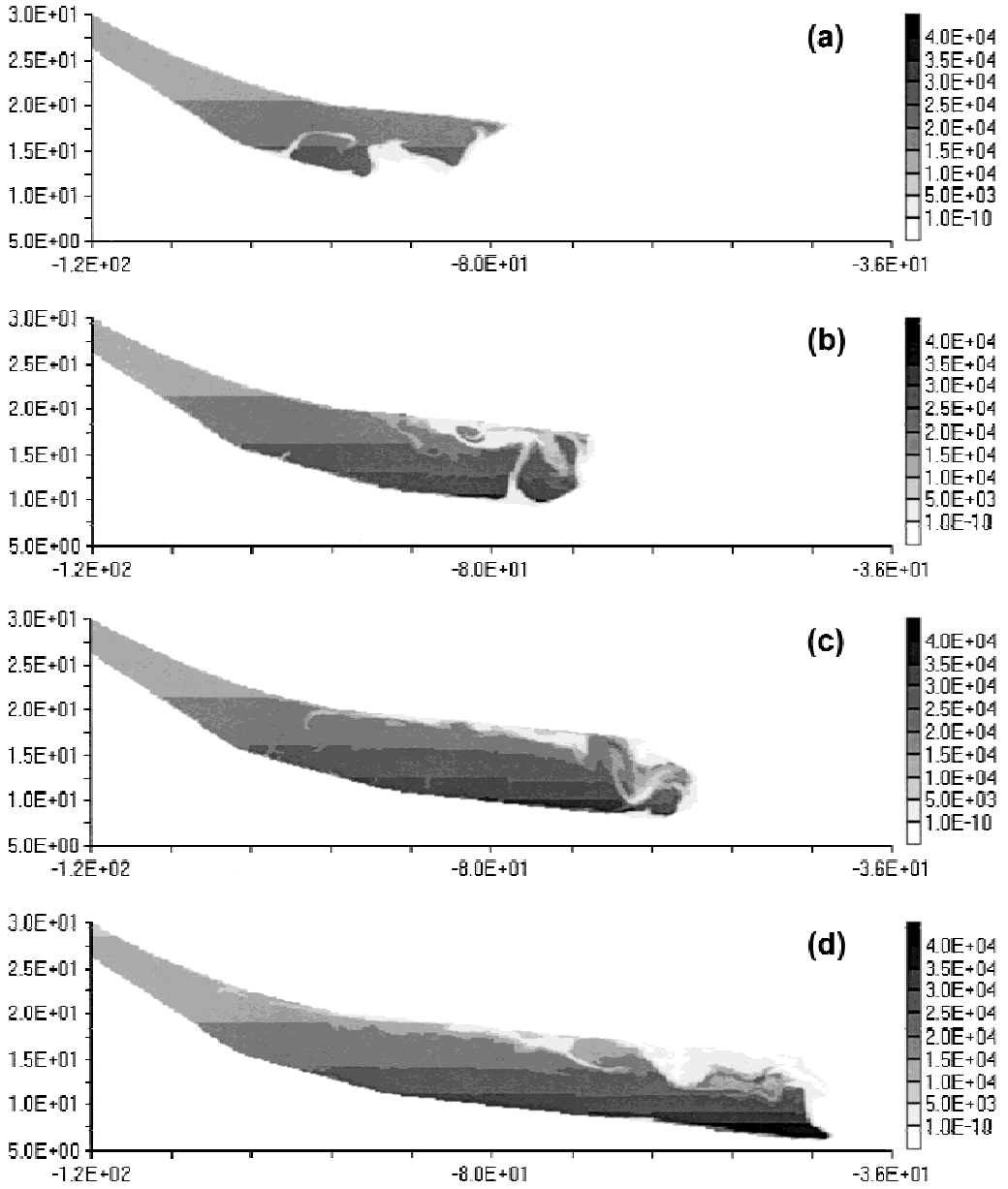

Fig. 4. Distribution of the magnetic field (Gs) at the times: (a) 5 μs, (b) 7.5 μs, (c) 10 μs, and (d) 12.5 μs.

velocity is approximately 5 cm/μs, because at these times the current reaches the maximum density near the holes in the internal electrode. When the current overcomes the maximum density the plasma velocity increases and to the time 12.5 μs achieves approximately 8 cm/μs.

ACKNOWLEDGMENTS

I am grateful to A.I. Zhitlukhin and V. Bakhtin for the experimental material they provided and want to thank Yu.I. Matveenko and M.A. Erokhin for the very useful discussions. This work was supported by the International Science and Technology Center (ISTC), Project No. 78.

REFERENCES

Bakhtin, V. & Zhitlukhin, A.I. (1998). Private communication.
Boris, J.P. & Book, D.L. (1976). *J. Comp. Phys.* **20**, 397.
Braginskii, S.L. (1965). *Review of plasma physics* **1** (New York: Consultant Bureau).
Potter, D.E. (1971). *Phys. Fluids* **14**, 1911.
Raman, R. *et al.* (1993). *Fusion Technology* **24**, 239.
Sidnev, V.V. *et al.* (1983). *VANT, ser. Termoyadernyi Sintez* **N2**, 12 (in Russian).
Yanenko, N.N. (1967). *Metod drobnyh shagov resheniya mnogomernyh zadach matematicheskoi fiziki* (Nauka, Novosibirsk, in Russian).

https://doi.org/10.1017/S0263034600182163 Published online by Cambridge University Press